

# Stair-Climbing Charts: on the optimal body height for quadruped robots to walk on stairs

Victor Barasuol, Sinan Emre, and Claudio Semini

Dynamic Legged Systems, Istituto Italiano di Tecnologia, Genoa/GE, 16163, Italy,  
name.surname@iit.it,  
dls.iit.it

**Abstract.** Quadruped robots have increasingly become one of the main choices when a mobile platform must be deployed to execute tasks in unstructured environments. Nowadays, their major applications are concentrated on monitoring and inspection inside industrial buildings, oil&gas platforms, and construction sites. In such environments, going up and down staircases are a common need and represent the most dangerous scenario where the robot locomotion is expected to be robust enough to prevent catastrophic damages in case of a fall. In this paper, we present a study on the robot's body height to maximize feasible footholds when walking on stairs. As per study results, this paper introduces the Stair Climbing Charts (SCCs), which describe the best robot height to climb stairs according to the robot's upper-leg length and lower-leg geometry, as well as the stair geometry (rise/go). Moreover, this paper presents a set of SCCs for various well-known quadruped robots, sold commercially or prototypes of academic research labs, and discusses the major differences between them.

**Keywords:** legged robots, quadruped locomotion, stair climbing

## 1 Introduction and State-of-the-Art

Due to their notorious ability to move on irregular terrains, quadruped robots have been increasingly adopted as mobile platforms to perform tasks like monitoring and inspection in unstructured environments. To name a few demanding environments, one can mention industrial buildings, oil&gas platforms, and construction sites. Regarding locomotion requirements, walking up and down staircases is essential to accomplish the task in all these scenarios. Therefore, the robot locomotion controller must be robust to plan safe footholds and be sufficiently reactive, to prevent falls that might be catastrophic in such a scenario.

Given the importance of safe locomotion on stairs, many researchers have paid attention to this problem. Most of the researchers have tackled the stair-climbing problem from the motion planning perspective. In [1], the authors propose an optimized static gait for quadruped robots to walk on stairs. According to their study, the optimal pose is determined to statically stand on the stairs.

Then a high-level planner adjusts the step length and maximizes stair-climbing capabilities. In [2], a dynamic locomotion strategy for quadruped stair walking adjusts the gait period and gait pattern during blind locomotion. The motion is executed by using an MPC controller to increase the locomotion robustness on stairs. In this work, the authors do not mention the adjustment of the body height.

A perception and control framework for autonomous stair climbing is proposed in [3], where the geometric information about the stairs is extracted to adjust the robot's velocity and footholds by an optimization algorithm. The motion is executed using an MPC controller. In [4] an adaptive vision-based strategy is proposed to generate dynamic gaits for stair-climbing. The approach makes use of the Capture Point technique based on the linear inverted pendulum model for motion stabilization. And in [5], instead, the authors propose a balance controller for stair climbing based on fuzzy logic. In all these works, the authors do not mention the influence of the robot's body height when performing locomotion on stairs.

Other studies on stair-climbing for quadruped robots regard the design of the quadruped machine itself. In [6], the authors present the design of a quadruped robot under stair parameter analysis and climbing capabilities. And a stair-climbing capability-based dimensional synthesis is introduced in [7, 8] for the design of a hexapod robot. In these last two works, the authors determine the leg and body lengths according to a target staircase and based on a pre-defined tripod gait.

Detecting the stair parameters is also very relevant to what regards stair-climbing since it allows the robot to adapt its motion and increase the locomotion robustness. In [9], the authors propose an algorithm to detect the dimensions of the stairs, by means of a stereo vision module with a line laser, for the path planning of a bipedal robot. Exploiting a 3D point cloud, instead, a stair detection method is proposed in [10]. In [11], authors proposed a real-time stairs geometric parameters estimation from a point cloud reconstructed from RGB-D data. And stair-mapping and stair-modeling are proposed in [12] also using point-cloud data.

Based on the literature review, we notice that there are very few papers assessing the impact of the robot body height for stair-climbing. At the same time, there are many proposed methods that allow for the online identification of stairs' geometric parameters to adjust the locomotion. Therefore, in this paper, we propose a stair-climbing analysis that culminates in a proposed Stair-Climbing Chart. Such a chart has the objective of assessing the robot's stair-climbing capabilities and guiding the control framework to set the body height that increases the locomotion robustness on stairs. Moreover, the proposed chart can be used to prevent the robot from attempting a risky stair-climbing or even as a tool to select the most appropriate quadruped robot model for a given stair geometry.

The paper is organized as follows. Section 2 presents the proposed method and its considerations to determine what is called the optimal body height for

stair climbing. In Sec. 3 we introduce the Stair Climbing Charts, which are a way of depicting the result analysis and guiding the choice for the robot climbing height. As a result, Stair Climbing Charts are computed for several robots and presented in Sec. 4. Section 5 closes the manuscript with final conclusions.

## 2 Computing the Optimal Height for Stair-Climbing

In this section, we describe the method used to determine what is the optimal height to perform locomotion on stairs, which is independent of gait parameters, leg sequence, or from considering a dynamic or static gait. Before introducing the definition of *optimal stair-climbing height*, we first describe how the robot models and the staircases are simplified and parameterized.

### 2.1 Assumptions and Definitions

Our analysis considers what is currently the most used kinematic configuration for quadruped robots, i.e., 3 degrees-of-freedom legs with the following sequential joints: hip adduction/abduction (HAA); hip flexion/extension (HFE); and knee flexion/extension (KFE). This configuration is found, for example, in various well-known research and commercial platforms [13], [14], [15], [16], [17], [18], [19], [20], [21]. Assuming that each HAA joint is very close to its zero position and that, during regular stair-climbing, it experiences negligible displacement, each leg is simplified to only the last two leg limbs (the upper leg and the lower leg, i.e. thigh and shank)<sup>1</sup>. Figure 1 depicts three-leg model approximations used in our analysis, which is performed on the robot’s sagittal plane. The most appropriate leg model is chosen in order to better approximate the lower-leg geometry of the robot under study.

The model illustrated in Fig. 1a is used to represent simple lower-leg designs like the one of our hydraulic quadruped robot HyQ [17]. Figure 1b and Figure 1c represent more complex lower-leg designs, such as the ones of robots like Anymal[13], Aliengo[14], and HyqReal [16]. The upper-leg length (distance between HFE and KFE joints) and the lower-leg length (distance between the knee joint and the foot) are denoted by  $l_1$  and  $l_2$ , respectively. For more complex designs, the lower-leg shape is approximated by segments  $s_i$  and corresponding bending angles  $\alpha_i$  (see Figures 1b and 1c). The foot is geometrically modeled as a circle of radius  $r$ . The HFE and KFE joint angles are represented, respectively, by  $\theta_1$  and  $\theta_2$ . All angles are measured positively using the right-hand rule convention.

For the staircase modeling, we consider two geometric parameters: the stair’s *Go*, which represents the horizontal length of one step, and the stair’s *Rise*, which represents the vertical length (or height) of one step. For the proposed analysis, it is assumed that the robot performs stair-climbing with constant body height  $h$ , which defines the hereafter called *motion line*. The motion line is parallel to

---

<sup>1</sup> Note that by considering the HAA joint at zero position the analysis already considers the HAA position that minimizes undesired lower leg collision with the stair edges.

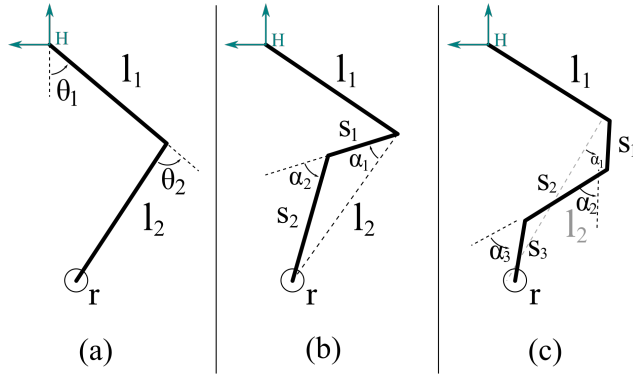


**Fig. 1.** Upper-leg and lower-leg model approximations: (a) one-segment shin model, (b) two-segment shin model, and (c) three-segment shin model.

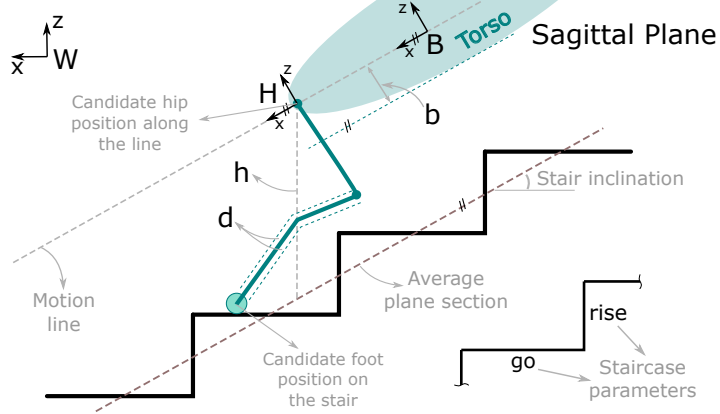


**Fig. 2.** Parameters, definitions, and concepts used to assess the optimal robot height for stair-climbing.

the stair inclination, which is computed according to its *Go* and *Rise* geometric parameters. Some reference frames are used to describe all the elements: the robot base frame  $B$ , the robot hip frame  $H$ , and the world/inertial frame  $W$ . To what concerns the mechanical shape of the lower leg and robot torso, the lower leg thickness is assumed uniform and approximated by  $d$  and the robot's belly thickness by  $b$ . Figure 2 illustrates all the parameters, definitions, and concepts involved in this proposed analysis.

As can be seen in Figure 2, the robot height  $h$  is measured as the vertical distance (parallel to the  $z$ -axis of the world frame) between the robot base frame  $B$  and the line represent the plane that approximates the stairs. Some other considerations are essential to the analysis scenario:

- The base frame and the hip frame have the same orientation with respect to the inertial frame  $W$ , i.e., there is no rotation between them;
- The hip  $z$  position in the coordinate frame  $B$  is zero. Note: in case this assumption is not representative of a robot design, it is sufficient to add the  $z$  distance of the hip w.r.t. to  $B$  as an offset on the computed optimal height;
- The robot is assumed to perform a straight trajectory along the stairs that is orthogonal to the line resulting from the intersection of the *Go* and *Rise* planes (i.e., the edges of the staircase).
- The robot pitch attitude is constant and such that the longitudinal robot axis ( $x$  coordinate of  $B$ ) is always parallel to the motion line.

## 2.2 Method Description and Definition of Optimal Height

The proposed analysis assesses the leg workspace regarding feasible foot contact positions on the stairs and the lower-leg collision with the stairs' edges and with the *Go* and *Rise* surfaces (which are represented by black solid lines in Fig. 2). To be more representative in the collision analysis, we add a distance margin  $d$  around the segments composing the simplified lower-leg model to approximate the thickness of the real lower-leg. In the same manner, we approximate the influence of the robot's belly by the distance margin  $b$  (see Fig. 2).

Our algorithm performs these two assessments for every pair of *candidate hip position*, along the motion line, and *candidate foot position* on the stairs (where the motion the line is defined according to a given stair-climbing height). Because of the geometric periodicity of the stairs, we perform the analysis over one single stair. More precisely, the projection of a candidate hip position<sup>2</sup> on the stairs  $x_h^w$  ranges from the position of an arbitrary stairs' edge to the next (i.e., the total hip horizontal displacement is equal to the *Go* parameter). Discrete positions between the two extreme candidate hip positions are considered for the assessment. Due to the same geometric property, the horizontal component of the candidate foot position on the stairs ranges by the same amount (i.e., by a *Go* distance), but in terms of location the horizontal component of the candidate foot position starts from  $x_h^w - Go/2$  until  $x_h^w + Go/2$ . Figure 3 depicts a series of assessments for a candidate hip position and various corresponding candidate foot positions.

Note that by taking into consideration a *Go* distance as the relative range for the candidate foot positions, we assume that the robot will not execute a step length larger than *Go* (this is the case for all the robots considered for analysis in Sec. 4).

Iterating on all the combinations of candidate hip positions along the motion line and corresponding candidate foot positions, we can assess how much a given stair-climbing height enables the robot to make successful foot-stairs contact. From this notion, we introduce the definition of a *valid stair-climbing height*:

---

<sup>2</sup> The hip position, described in the world sagittal plane, is represented by the pair of coordinates  $(x_h^w, z_h^w)$ .

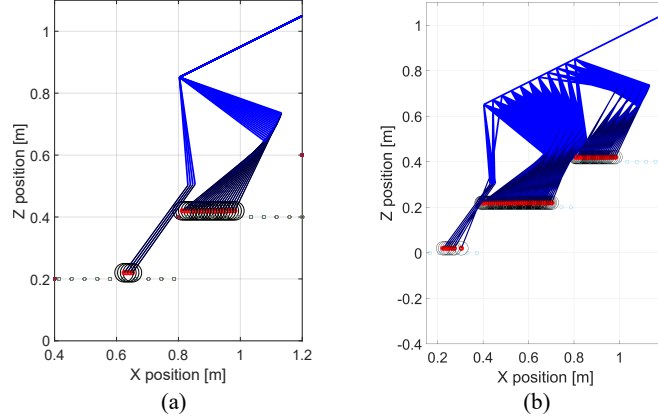


**Fig. 3.** Examples of body height assessment along the motion line: a) partial assessment depicting only one candidate hip position along the motion line and its respective candidate foot positions. b) complete assessment with all candidate hip and foot positions. Both figures depict only the successful configurations.

**Definition of valid stair-climbing height:** *it is a body height that enables the robot, at any candidate hip position, to make at least  $n$  successful foot-stair contacts.*

This minimum number of successful contacts  $n$  is an input parameter for the analysis and it is tightly related to the distance between consecutive candidate footholds (that depends on the number of foot candidates set to be assessed inside the range). I.e., the smaller the distance between each consecutive candidate foot position, the larger the  $n$  value.

Finally, the definition of optimal stair-climbing height (or simply optimal height) can be introduced:

**Definition of optimal stair-climbing height:** *it is the valid stair-climbing height, kept along the whole staircase crossing, that maximizes the minimum number of successful foot-stair contacts.*

In summary, the proposed method focuses on determining a body height that maximizes the locomotion robustness for stair-climbing by providing a pose that allows the robot to always have locations to make safe contact with the stairs.

In the next section, we introduce the Stair-Climbing Charts, a way to depict all the results from this assessment to help to understand the robot's kinematic capabilities for stair-climbing tasks.

### 3 Stair-Climbing Charts

In this section, we introduce the Stair-Climbing Charts (SCCs). A SCC is a way of synthesizing the results from the method presented in Sec 2, depicting them such that it is easier to conclude about the robot's capabilities regarding stair climbing. Considering a set of given leg parameters, the chart displays two relevant pieces of information: 1) the optimal stair-climbing height and 2) its corresponding minimum number of successful candidate foot positions in terms of percentage of the  $Go$  length. All this information is plotted in terms of  $Go$  and  $Rise$  parameters which are the dimensions of the stair. Therefore, the chart is a sort of description composed of two 2.5D maps superposed to each other, where the optimal height is plotted as a colormap (first map) and the corresponding minimum number of successful candidate foot positions is plotted as contour lines (second map). An example of SCC is depicted in Fig. 4.

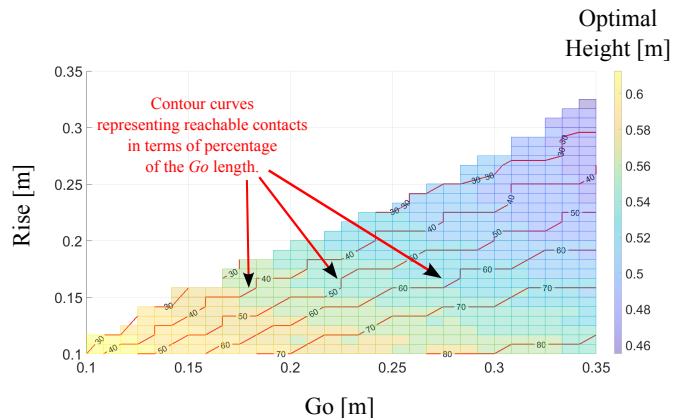


**Fig. 4.** Example of stair-climbing chart computed for the HyQ robot. The color map indicates the optimal height and the contour lines provide information about the corresponding minimum number of successful candidate foot positions (reachable contacts).

With a SCC, one can conclude whether a given robot is capable to perform stair-climbing for certain staircase parameters and how safe the locomotion can be. The more accurate the leg geometric model used in the assessment, and more refined the distance between candidate positions, the more accurate a SCC becomes.

Given the geometric features of the stairs and the way the algorithm iterates (progressing sequentially from one extreme to another of each candidate hip/foot position range), a SCC presents a smooth shape without peaks and holes inside the region with valid optimal heights. This even allows one to compute a plane that approximates optimal heights, extracting an equation to be used online to adapt the body height once the staircase parameters are detected. Another way would be to consider a look-up table with the complete data from the chart.

## 4 Results

In this section, we present the SCC for much well-known research and commercial quadruped robots, being them: Aliengo [14], Anymal C [13], B1 [18], Hound [19], HyQ [17], HyQReal [16], MiniCheetah [15], Solo [20], and Spot [21]. The lower leg model approximation chosen for each of the candidate robots are depicted in Figure 5, and each corresponding set of leg model parameters, following the definitions introduced in Sec. 2.1, are reported in Table 1. The \* symbol after the parameter value means that the parameter was assumed for the sake of comparison. The other values that complete the table were extracted from available robot urdf files or robot datasheets.

**Table 1.** Parameters of the leg simplified models depicted in Fig. 5.

Robot	Leg Model Parameters												
	$l_1[m]$	$l_2[m]$	$s_1[m]$	$s_2[m]$	$s_3[m]$	$r[m]$	$d[m]$	$b[m]$	$\alpha_1[^\circ]$	$\alpha_2[^\circ]$	$\alpha_3[^\circ]$	HFE Limit $[^\circ]$	KFE Limit $[^\circ]$
AlienGo	0.25	0.25	0.22	0.031	-	0.025	0.015	0.075*	-4	0	-	-120 to 240	-159 to -37
Anymal	0.285	0.35	0.165	0.24	-	0.024	0.02*	0.1*	-40	0	-	$\pm 360$	$\pm 360$
Hound	0.33	0.35	-	-	-	0.025	0.02*	0.11*	-	-	-	$\pm 360$	$\pm 160$
HyQ	0.35	0.35	-	-	-	0.02	0.02	0.163	-	-	-	-70 to +50	-140 to -20
HyqReal	0.36	0.38	0.0716	0.26	0.068	0.03	0.015	0.25	37	-56	0	$\pm 110$	$\pm 133$
MiniCheetah	0.21	0.18	-	-	-	0.015	0.01*	0.045*	-	-	-	$\pm 270$	$\pm 155$
Solo	0.16	0.16	-	-	-	0.013	0.01	0.03*	-	-	-	$\pm 360$	$\pm 360$
Spot	0.38	0.38	0.14	0.22	0.05	0.03	0.015	0.096*	0	-15	20	$\pm 91$	-160 to -14
B1	0.33	0.33	0.3	0.036	-	0.025	0.015*	0.15*	-4	0	-	$\pm 110^*$	-159* to -37*

After processing the height assessment for all the candidate robots, their stair-climbing charts are depicted in Fig. 6. We set a minimum number of successful candidate foot positions  $n$  that corresponds to at least 20% of the  $Go$  surface (i.e., body heights that have such corresponding number lower than 20% are considered inadequate for stair climbing).

As expected, smaller robots (like Solo and MiniCheetah) are able to stair-climb a smaller set of staircase parameters in comparison to larger robots (like B1, HyQReal, and Anymal C). For smaller robots, the *Rise* range value is not primarily limited by their leg workspace but, instead, by their belly thickness. An interesting result regards the comparison between robots of similar size but different lower leg configurations. It is possible to see, from both the colormap and the contour lines, how lower-leg designs with bent shapes can substantially increase the minimum number of successful candidate foot positions for each optimal stair-climbing height. For example, considering the pair  $(Go, Rise) = (0.28, 0.16)$ , Anymal's optimal stair-climbing height is about 0.42 m reaching about 93% of the  $Go$  surface, Spot robot is about 0.58 m with 80%, and HyQReal is about 0.53 with 60%. Robots with lower-leg designs with bent shapes also cope better with a larger range of stairs that have a lower  $Go$  value. For example, for a  $Go = 0.15$  m, Anymal can deal with *Rise* values up to about 0.25 m, Spot up to 0.2 m, and B1 up to 0.15 m. For the robots that have lower legs with more straight shapes, like Hound, HyQ, and HyQReal, *Rise* values are up to 0.18 m, 0.16 m, and 0.14 m, respectively.

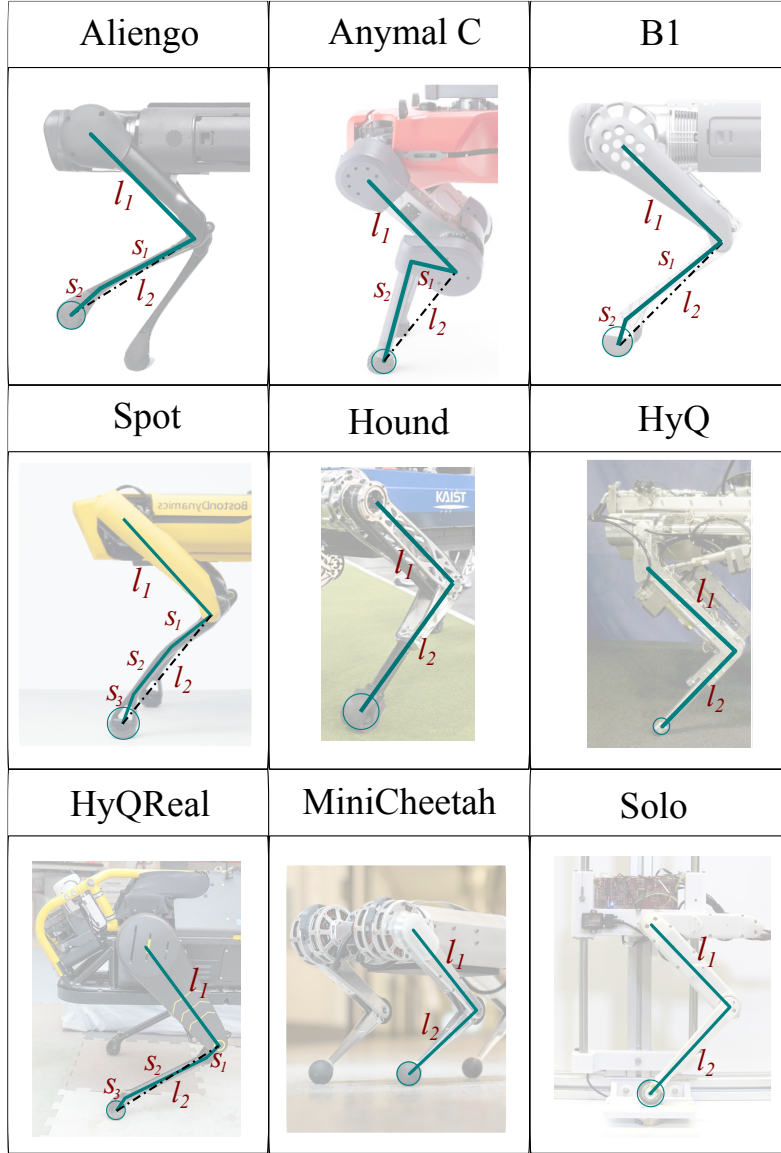


**Fig. 5.** Research and commercial quadruped robots considered for the generation and comparison of stair-climbing charts.

Some parts in the chart may present a relatively abrupt change in the value of the optimal height for staircase parameters that are neighbors. This is mainly caused by the discretization steps chosen to generate the charts with a shorter computational time. Reducing the distance between candidate hip and foot positions are very likely to remove such abrupt variations.

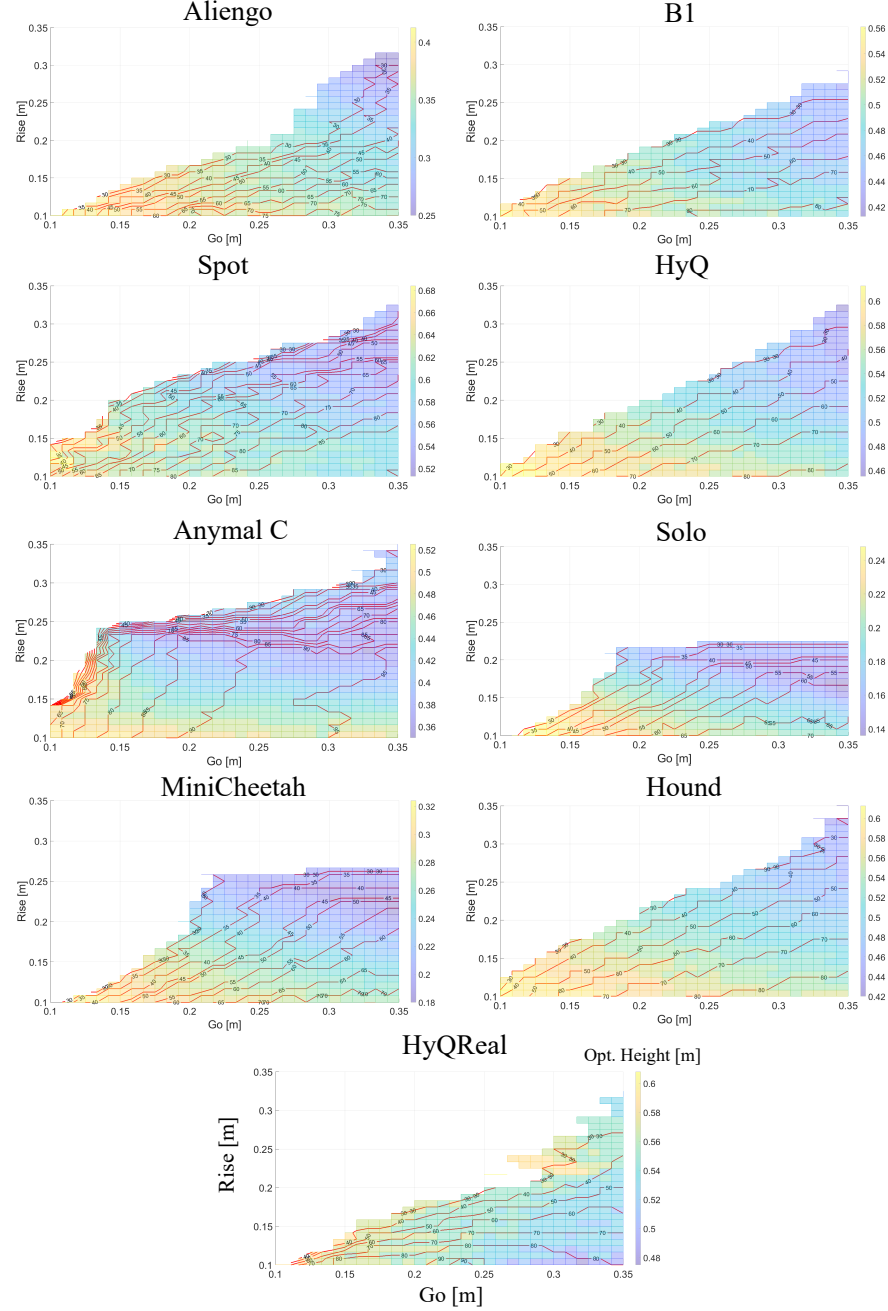


**Fig. 6.** Resulting stair-climbing charts for some of the well-known commercial and non-commercial quadruped robots.

## 5 Conclusions

In this paper, we introduced the Stair-Climbing Chart, a new chart to assess the robot's capabilities and available locomotion robustness for the quadruped locomotion when performing stair-climbing. The chart provides information about the optimal stair climbing heights, for a given robot's upper and lower leg parameters, with respect to the staircase parameters *Rise* and *Go*. Since the analysis is bounded to kinematic and leg collision, and focused on assessing reachable footholds at touch-down, the results are independent of gait parameters, leg sequence, or motion direction. The information from the chart can be exploited during locomotion to online adapt the body height once the staircase parameters are known or detected.

The paper presented the SCC for several research and commercial quadruped robots and major differences were highlighted. In future work, we intend to refine the analysis and all charts with a more accurate geometric approximation for the robot legs and make them available to the community.

## References

1. Linqi Ye, Yaqi Wang, Xueqian Wang, Houde Liu, and Bin Liang. Optimized static gait for quadruped robots walking on stairs. In *2021 IEEE 17th International Conference on Automation Science and Engineering (CASE)*, pages 921–927, 2021.
2. Daekeun Yoon, Baekchul Kim, Ikhee Jo, and Woong Jeong. A dynamic locomotion strategy for stair walking of a quadruped robot. In *2021 18th International Conference on Ubiquitous Robots (UR)*, pages 223–227, 2021.
3. Shuhao Qi, Wenchun Lin, Zeyun Hong, Hua Chen, and Wei Zhang. Perceptive autonomous stair climbing for quadrupedal robots. In *2021 IEEE/RSJ International Conference on Intelligent Robots and Systems (IROS)*, pages 2313–2320, 2021.
4. Qixing Liang, Bin Li, Yiming Xu, Landong Hou, and Xuewen Rong. Vision-based dynamic gait stair climbing algorithm for quadruped robot. In *2022 IEEE International Conference on Robotics and Biomimetics (ROBIO)*, pages 1390–1395, 2022.
5. Alvin Teguh Budi Antok, Adytia Darmawan, Ali Husein Alasiry, Hendhi Hermawan, Eko Henfri Binugroho, Bayu Sandi Marta, Ibnu Kresno Wibowo, Aldifa Julian, and Andre Faqih Ilham Suparman. Quadruped robot balance control for stair climbing based on fuzzy logic. In *2021 International Electronics Symposium (IES)*, pages 552–557, 2021.
6. Ganesh Kale, Sanjay Gandhe, Pravin Dhulekar, and Sushant Pawar. Designing a quadruped with stair parameter analyzing and climbing capability. In *2015 International Conference on Computing Communication Control and Automation*, pages 546–550, 2015.
7. Huayang Li, Chenkun Qi, Xianbao Chen, Liheng Mao, Yue Zhao, and Feng Gao. Stair climbing capability-based dimensional synthesis for the multi-legged robot. In *2021 IEEE International Conference on Robotics and Automation (ICRA)*, pages 2950–2956, 2021.
8. Huayang Li, Chenkun Qi, Liheng Mao, Yue Zhao, Xianbao Chen, and Feng Gao. Staircase-climbing capability-based dimension design of a hexapod robot. *Mechanism and Machine Theory*, 164:104400, 2021.

9. A. Albert, M. Suppa, and W. Gerth. Detection of stair dimensions for the path planning of a bipedal robot. In *2001 IEEE/ASME International Conference on Advanced Intelligent Mechatronics. Proceedings (Cat. No.01TH8556)*, volume 2, pages 1291–1296 vol.2, 2001.
10. Arnab Sinha, Panagiotis Papadakis, and Mohan Rajesh Elara. A staircase detection method for 3d point clouds. In *2014 13th International Conference on Control Automation Robotics Vision (ICARCV)*, pages 652–656, 2014.
11. Xiaoming Zhao, Weihai Chen, Xing Yan, Jianhua Wang, and Xingming Wu. Real-time stairs geometric parameters estimation for lower limb rehabilitation exoskeleton. In *2018 Chinese Control And Decision Conference (CCDC)*, pages 5018–5023, 2018.
12. Seungjun Woo, Jinjae Shin, Yoon Haeng Lee, Young Hun Lee, Hyunyong Lee, Hansol Kang, Hyouk Ryeol Choi, and Hyungpil Moon. Stair-mapping with point-cloud data and stair-modeling for quadruped robot. In *2019 16th International Conference on Ubiquitous Robots (UR)*, pages 81–86, 2019.
13. M. Hutter, C. Gehring, A. Lauber, F. Gunther, C. D. Bellicoso, V. Tsounis, P. Fankhauser, R. Diethelm, S. Bachmann, M. Bloesch, H. Kolenbach, M. Bjelonic, L. Isler, and K. Meyer. Anymal - toward legged robots for harsh environments. *Advanced Robotics*, 31(17):918–931, 2017.
14. Unitree’s aliengo robot. <https://www.unitree.com/en/aliengo/>. Accessed: 08/05/2023.
15. Benjamin Katz, Jared Di Carlo, and Sangbae Kim. Mini cheetah: A platform for pushing the limits of dynamic quadruped control. In *2019 International Conference on Robotics and Automation (ICRA)*, pages 6295–6301, 2019.
16. Claudio Semini, Victor Barasoul, Michele Focchi, Chundri Boelens, Mohamed Emara, Salvatore Casella, Octavio Villarreal, Romeo Orsolino, Geoff Fink, Shamel Fahmi, Gustavo Medrano-Cerda, Dhinesh Sangiah, Jack Lesniewski, Kyle Fulton, Michel Donadon, Mike Baker, and Darwin G. Caldwell. Brief introduction to the quadruped robot hyqreal. In *Italian Conference on Robotics and Intelligent Machines (I-RIM)*, pages 1–2, Rome, Oct 2019.
17. Claudio Semini, Nikos G. Tsagarakis, Emanuele Guglielmino, Michele Focchi, Ferdinando Cannella, and Darwin G. Caldwell. Design of hyq - a hydraulically and electrically actuated quadruped robot. *IMechE Part I: Journal of Systems and Control Engineering*, 225(6):831–849, 2011.
18. Unitree’s b1 robot. <https://shop.unitree.com/products/unitree-b1>. Accessed: 08/05/2023.
19. Young-Ha Shin, Seungwoo Hong, Sangyoung Woo, JongHun Choe, Harim Son, Gijeong Kim, Joon-Ha Kim, KangKyu Lee, Jemin Hwangbo, and Hae-Won Park. Design of kaist hound, a quadruped robot platform for fast and efficient locomotion with mixed-integer nonlinear optimization of a gear train. In *2022 International Conference on Robotics and Automation (ICRA)*, pages 6614–6620, 2022.
20. Felix Grimminger, Avadesh Meduri, Majid Khadiv, Julian Viereck, Manuel Wüthrich, Maximilien Naveau, Vincent Berenz, Steve Heim, Felix Widmaier, Thomas Flayols, Jonathan Fiene, Alexander Badri-Spröwitz, and Ludovic Righetti. An open torque-controlled modular robot architecture for legged locomotion research. *IEEE Robotics and Automation Letters*, 5(2):3650–3657, 2020.
21. Boston dynamics’ spot robot. <https://www.bostondynamics.com/products/spot>. Accessed: 08/05/2023.